World Applied Sciences Journal 11 (1): 12-17, 2010
ISSN 1818-4952

Simulation of Static Characteristics of Self-Assembled Quantum Dot Lasers

[1]D. Ghodsi Nahri and [2]A.S. Naeimi

[1]Department of Physics, Faculty of Science,
Islamic Azad University, Mashhad Branch, Mashhad, Iran
[2]Islamic Azad University, Aliabad Katoul Branch, Iran

Abstract: Static-characteristics of self-assembled quantum-dot (SAQD) lasers are treated solving the rate equations numerically using fourth-order Runge-Kutta method. Energy level and size distributions of self-assembled quantum-dots are considered and their effects on Static-characteristics are investigated. Simulation results of static-characteristics show that nonlinearity appears in light-current characteristics whereas homogeneous broadening becomes equal to inhomogeneous broadening. Slope-efficiency increases as the homogeneous broadening heightens up to inhomogeneous broadening. Exceeding the homogeneous broadening from inhomogeneous broadening results in degradation of light-current characteristics. In fact, SAQD laser has the best performance when homogeneous broadening is equal to inhomogeneous broadening. Light-current characteristics degrade and threshold current increases as inhomogeneous broadening enhances. We also investigate the effects of quantum dot coverage on the laser performance and show that there is a threshold coverage for quantum-dots to begin lasing and an optimum quantum-dot coverage in which the SAQD lasers operate with lowest possible threshold current and maximum output power. In addition, we show that differential gain degrades as initial relaxation time increases and recombination times in quantum dots and wetting layer decrease. Consequently, relaxation oscillation frequency and modulation bandwidth decline.

Key words: Quantum-dot laser · Inhomogeneous and homogeneous broadenings · Static-characteristics

INTRODUCTION

Semiconductor lasers with quantum dots (nanostructures) in their active regions are expected to exhibit many superior properties, such as ultralow threshold currents, temperature insensitive andhigh-speed operation, high optical gain, broad modulation bandwidth and narrow spectrum linewidth due to three dimensional electronic confinement that results in completely discrete energy spectrum and allow the investigation of typical effects of atomic physics in a solid state environment [1-4]. However, we know that actual quantum dots (Qds) do not always satisfy our expectation because of the energy level broadening (homogeneous broadening) and size distributions (inhomogeneous broadening) and phonon bottleneck. Thus, for an accurate comprehension of quantum dot laser diode (QD-LD) performance, we must take into account all these actual aspects of QDs [5].

In this paper, simulating model of QD laser performance are described based on rate equations. We solve the rate equations considering homogeneous and inhomogeneous broadenings of the linear optical gain numerically using fourth-order Runge-Kutta method for a specific InGaAs/GaAs self-assembled quantum dot laser (SAQD-LD). We simulate static response and analyze the effects of inhomogeneous and homogeneous broadenings on static-characteristics. We also consider QD coverage as a variable parameter and inspect its effect on the laser performance. Finally, the effects of recombination times and initial relaxation time (phonon-bottleneck) are also treated on optical gain-current characteristics.

Simulation Model: Solving rate equations for carrier and photons is the most accurate way to treat static and dynamic characteristics in lasers. Fig. 1 illustrates the energy diagram of the conduction band of the quantum dot laser active region and diffusion, relaxation, recombination and escape processes of carriers [6, 7].

Corresponding Author: Davoud Ghodsi Nahri, Department of Physics, Faculty of Science, Islamic Azad University, Mashhad Branch, Mashhad, Iran, E-mail: davodghn@yahoo.com.

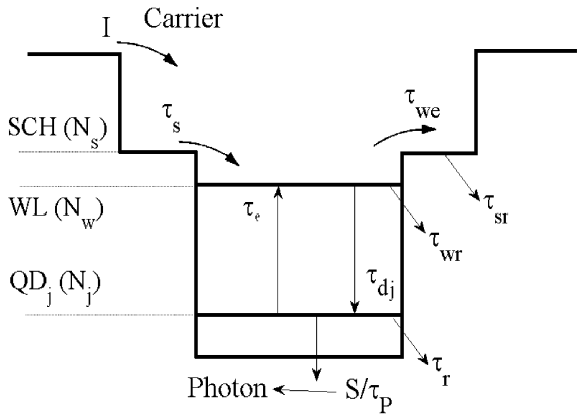

Fig. 1: Energy diagram of the laser-active region and diffusion, recombination and relaxation processes

We consider an exciton model. It means that both an electron and a hole relax into the ground state simultaneously to form an exciton. We assume that only a single discrete electron and hole ground state is formed inside the QD and the charge neutrality always holds in each QD.

We divide the QD ensemble into *j=1, 2,..., 2M+1* groups, depending on their resonant energy for the interband transition, over the longitudinal cavity photon modes. $j = M$ corresponds to the group and the mode at E_{cv}. We take the energy width of each group equal to the mode separation of the longitudinal cavity photon modes which equals to

$$\Delta E = ch/(2n_r L_{ca}) \tag{1}$$

Where L_{ca} is the cavity length. The energy of the *j*th QDs group is represented by

$$E_j = E_{cv} - (M - j)\Delta E \tag{2}$$

Where $j = 1,2,...,2M + 1$. The QD density of *j*th group is given as

$$N_D G_j = N_D G(E_j - E_{cv})\Delta E \tag{3}$$

Where N_D is the volume density of QDs and the energy fluctuation of QDs is given as

$$G\left(E_j - E_{cv}\right) = \frac{1}{\sqrt{2\pi}\xi_0}\exp\left[-\left(E_j - E_{cv}\right)^2 \Big/ 2\xi_0^{\,2}\right] \tag{4}$$

that takes a Gaussian distribution function and Whose FWHM is given by $\Gamma_0 = 2.35\xi_0$. We consider N_j as the carrier number in *j*th QDs group, According to Pauli's exclusion principle, the occupation probability in the ground state of the *j*th QDs group is defined as

$$P_j = N_j \Big/ \left(2N_D V_a G_j\right) \tag{5}$$

Where $V\alpha$ is the total active region volume.

The rate equations are as follows [5-9]

$$dN_s/dt = I/e - N_s/t_s - N_s/t_{sr} + N_w/t_{we} \tag{6}$$

$$dN_w/dt = N_s/t_s + \sum_j N_j/t_e D_g - N_w/t_{wr} - N_w/t_{we} - N_w/\overline{t}_d \tag{7}$$

$$dN_j/dt = N_w G_j/t_{dj} - N_j/t_r - N_j/t_e D_g - \frac{cG}{n_r}\sum_m g^{(l)} S_m \tag{8}$$

$$dS_m/dt = \beta N_j/t_r + \frac{cG}{n_r}\sum_j g^{(l)} S_m - S_m/t_p \tag{9}$$

Where N_s, N_w and N_j are the carrier number in SCH layer, wetting layer (WL) and *j*th QDs group, respectively, S_m is the photon number of mth mode, where *m=1,2...2M+1*, *I* is the injected current, G_j is the fraction of the *j*th QDs group type within an ensemble of different dot size populations, e is the electron charge, D_g is the degeneracy of the QD ground state without spin, β is the spontaneous-emission coupling efficiency to the lasing mode. The related time constants are, τ_s diffusion in the SCH region, τ_{sr} carrier recombination in the SCH region, τ_{we} carrier reexcitation from the WL to the SCH region, τ_{wr} carrier recombination in the WL, τ_{dj} carrier relaxation into the *j*th QDs group, τ_r carrier recombination in the QDs, τ_r photon lifetime in the cavity, The average carrier relaxation time, $\overline{\tau}_d$ is given as

$$\overline{t}_d^{\,-1} = \sum_n t_{dn}^{\,-1} G_n = \sum_n t_o^{\,-1}(1 - P_n) G_n \tag{10}$$

Where τ_o is the initial carrier relaxation time. The photon lifetime in the cavity is

$$t_p^{\,-1} = \left(c/n_r\right)\left[\alpha_i + \ln\left(1/R_1R_2\right)\Big/\left(2L_{cav}\right)\right] \tag{11}$$

Where R_1 and R_2 are the cavity mirror reflectivities and α_i is the internal loss.

The linear optical gain which the *j*th QDs group gives to the *m*th mode photons is represented by

Table 1: Parameters Used for Simulation of Ingas/gaas Saqd-Ld [6]

Parameter		Value
R	Radius of QD	$8nm$
h	Height of QD	$8nm$
E_{cv}	Interband transition energy	$1eV$
V_D	Volume of QD	$\pi R^2 h$
ξ	Coverage of QDs	20%
N_W	Number of QD layer	3
Γ	Optical confinement factor	4%
R_1,R_2	Mirror reflectivities	30%, 90%
α	Internal loss	$6cm^{-1}$
d	Stripe width	$10\mu m$
$V\alpha$	is the total active region volume	2.16×10^{-16}
τ_p	Photon cavity lifetime	$8.8ps$
L_{cav}	Cavity length	$900\mu m$
Γ_0	FWHM of inhomogeneous broadening	$20meV$
τ_0	Initial carrier relaxation lifetime	$10ps$
Δ	Spin-orbit interaction energy	$0.35eV$
m^*_e	Electron effective mass	$0.04m_0$
β	Spontaneous-emission coupling efficiency	10^{-4}
n_r	Refractive index	3.5
E_g	Band gap of bulk semiconductor	$0.8eV$
τ_s	Diffusion lifetime in the SCH region	$15ps$
τ_{WR}	Carrier recombination lifetime in the WL	$3ns$
τr	Carrier recombination lifetime in the QDs	$2.8ns$

$$g_{mj}^{(1)} = \frac{2pe^2 hN_D}{cn_r e_0 m_0^2} \frac{\left|P_{cv}^s\right|^2}{E_{cv}} \left(2P_j - 1\right) G_j B_{cv}\left(E_m - E_j\right) \tag{12}$$

Where n_r is the refractive index, $|P^{\sigma}_{cv}|^2$ is the transition matrix element, E_{cv} is the interband transition energy. The linear optical gain shows the homogeneous broadening of a Lorentz shape as

$$B_{cv}\left(E_m - E_j\right) = \frac{h\gamma_{cv}/\pi}{\left(E_m - E_j\right)^2 + \left(h\gamma_{cv}\right)^2} \tag{13}$$

Where whose FWHM is given as $2\hbar\gamma_{cv}$ with polarization dephasing or scattering rate γ_{cv} The transition matrix element is given as

$$\left|P_{cv}^{\sigma}\right|^2 = \left|I_{cv}\right|^2 M^2 \tag{14}$$

Where I_{cv} represents the overlap integral between the envelope functions of an electron and a hole and

$$M^2 = \frac{m_0^2}{12m_e^*} \frac{E_g(E_g + \Delta)}{E_g + 2\Delta/3} \tag{15}$$

derived by the first-order k.p interaction between the conduction band and valence band. Here, E_g is the band gap of bulk material, m^*_e is the electron effective mass, Δ is the spin-orbit interaction energy of the QD material. Equation (14) holds as long as we consider QDs with a nearly symmetrical shape.

The coverage of QDs which is related to density and volume of QDs, V_D, is given as

$$\xi = N_D V_D \tag{16}$$

The laser output power of the mth mode is also given as

$$I_m = \hbar\omega_m cSm \text{ In } (1/R)/2L_{cav}) \tag{17}$$

Where ω_m is the emitted photon frequency and R is R_1 or R_2.

We solved the rate equations numerically using fourth-order Runge-Kutta method to simulate light-current characteristics and optical gain profile. The system reaches the steady-state after finishing the relaxation oscillation. We assume that all the carriers are injected into the WL, i.e., $\tau_{sr} = \tau_{we} = \infty$ and do not consider the thermal carrier escape time, i.e., $\tau_e = \infty$. It is also assumed that QDs have a cylindrical shape. The parameters we used at simulation are listed in Table 1 [6].

Simulation Results: Fig. 2 shows light-current (L-I) characteristics of the mentioned self-assembled QD laser diode (SAQD-LD) for FWHM of inhomogeneous broadening $\Gamma_0 = 20meV$ at (a) $\hbar\gamma_{cv}$ = 2, 4.5, 5, 5.5 and $6.5meV$, (b) $\hbar\gamma_{cv}$ = 5, 7, 10 and $20meV$ and also, FWHM of inhomogeneous broadenings (c) $\Gamma_0 = 30meV$ at $\hbar\gamma_{cv}$ = 7, 10, 15 and $20meV$ and (d) $\Gamma_0 = 40meV$ at $\hbar\gamma_{cv}$ = 8 and| $10meV$.

As we can see from Fig. 2, with increase of homogeneous broadening, non- linearity appears at L-I characteristics and continues whereas the homogeneous broadening nearly becomes equal to inhomogeneous broadening. For large homogeneous broadenings, near to or larger than inhomogeneous broadening, output power increases infinitely as the injected current elevates. Besides, Slope efficiency (external quantum differential efficiency) heightens as the homogeneous broadening increases up to the inhomogeneous broadening (Fig. 2 (a) and Fig. 2(b)). In addition, when the homogeneous broadening exceeds the inhomogeneous broadening, static-characteristics degrade (Fig. 2(a) and Fig. 2(b)).

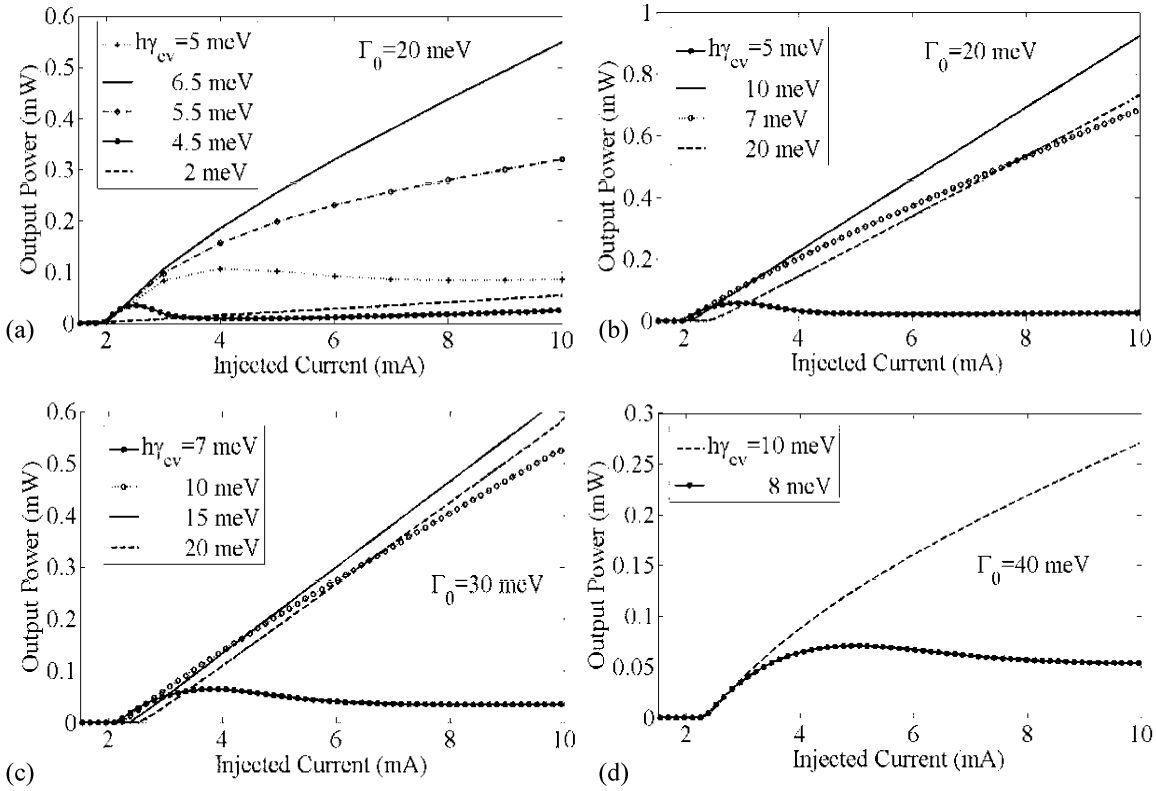

Fig. 2: light-current characteristics of SAQD-LD for FWHM of inhomogeneous broadening $\Gamma_0 = 20meV$ at (a) $\hbar\gamma_{cv} = 2$, 4.5, 5, 5.5, 6.5*meV* and (b) $\hbar\gamma cv = 2$, 7, 10, 20*meV* and also FWHM of inhomogeneous broadenings (C) $\Gamma_0 = 30meV$ at $\hbar\gamma_{cv} = 7$, 10, 15, *20meV* and (d) $\Gamma_0 = 40meV$ at $\hbar\gamma_{cv} = 8$ and 10*meV*.

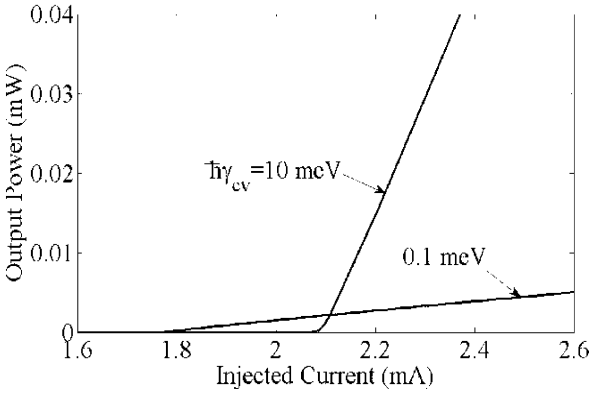

Fig. 3: Output power as a function of injected current for homogeneous broadening 0.2 and 20 meV

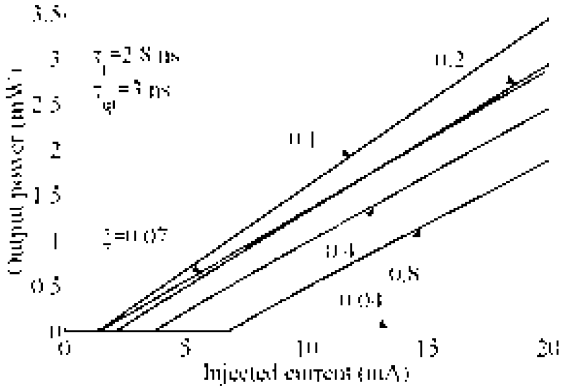

Fig. 4: Shows L-I characteristics for QD coverage as a variable parameter ξ = 0.04, 0.07, 0.1, 0.2, 0.4 and 0.8.

Furthermore, Fig. 2 shows that slope efficiency decreases and threshold current also elevates with enhancement of inhomogeneous broadening as a result of decreasing the central group DOS. In some cases such as Fig. 2(a) for FWHM of homogeneous broadening 9 meV and at I= 2.5 mA or for FWHM of homogeneous broadening 10 meV and at I=4 mA, all of the central group DOS occupies and the output power reaches its maximum amount, then, it decreases as the injected current increases, as a result of emitting of central group carriers within other modes.

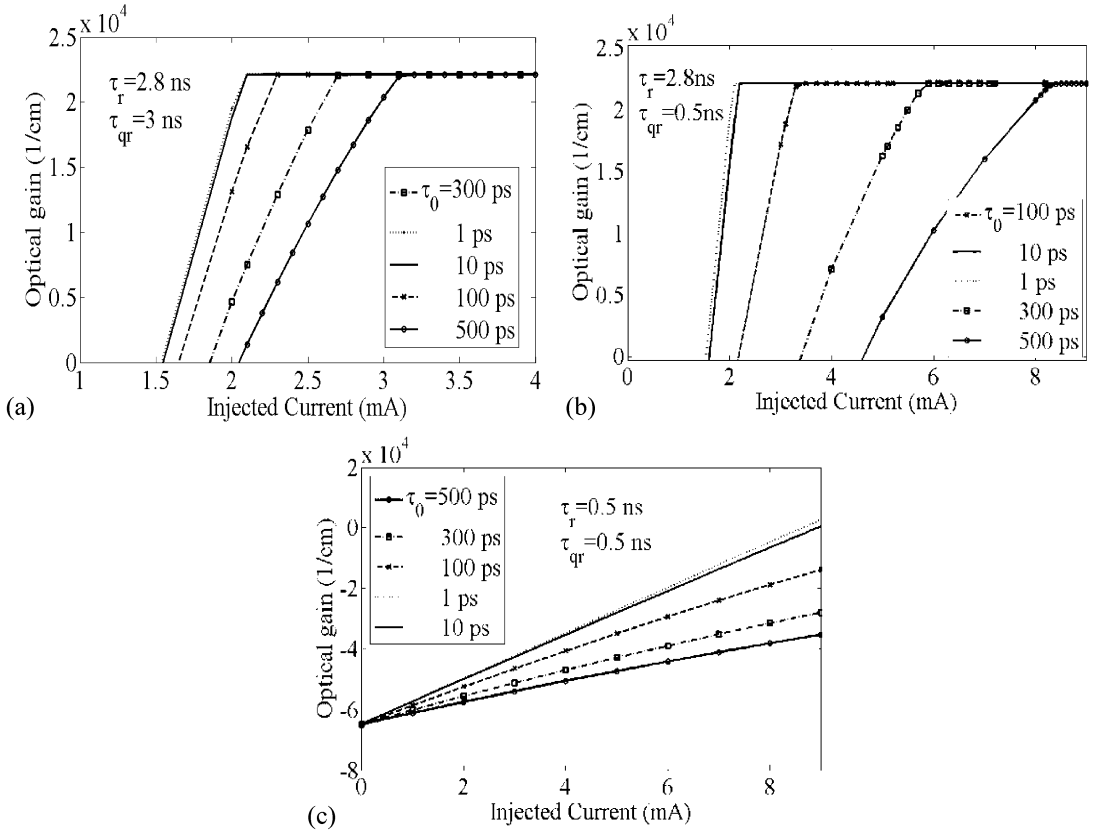

Fig. 5: Optical gain-current characteristics of SAQD-LD for different initial relaxation times τ_0 = 1, 10, 100, 300 and 500*ps* at different recombination times (a) τ_r = 2.8*ns*, τ_{qr} = 3*ns*, (b) τ_r = 2.8$_{ns}$, τ_{qr} = 0.5 *ns* and (c) τ_r = 0.5*ns*, τ_{qr} = 0.5*ns*.

Threshold current increases as the homogeneous broadening increases owing to elevating density of states (DOS) of the central group. This fact is revealed clearly in Fig. 3 where L-I characteristics is shown for homogeneous broadening 0.2 and 20 meV.

We can conclude that the SAQD laser has its best performance when homogeneous broadening is equal to inhomogeneous broadening.

Fig. 4. Shows L-I characteristics for QD coverage as a variable parameter ξ = 0.04, 0.07, 0.1, 0.2, 0.4 and 0.8.

As shown in Fig. 4, with increase of QD coverage from 0.1, threshold current increases owing to enhancing the number of QDs or the QD volume (the number of energy levels) and as a result, the need for more carriers to provide populationinversion. Besides, output power and slope efficiency decline due to decreasing occupation probability and accordingly, increasing the relaxation time. We also see that a threshold QD coverage exists that enables output photons to overcome losses and to generate laser emission. It is clearly revealed that the QD coverage 0.1 has the best L-I characteristics and the lowest threshold current. It is concluded that there is an optimum QD coverage.

Fig. 5 shows optical gain-current characteristics of SAQD-LD for different initial relaxation times τ_0 = 1. 10, 100, 300 and 500 *ps* at different recombination times in QDs and WL (a) τ_r = 2.8*ns*, τ_{qr} = 3*ns*, (b) τ_r = 2.8*ns*, τ_{qr} = 0.5*ns* and (c) τ_r = 0.5*ns*, τ_{qr} = 0.5*ns*.

Optical gain increases to the threshold gain and then fixes with enhancement of injected current. Actually, what happens when the current is increased to a value above threshold is that the carrier density and optical gain initially (for on the order of a nanosecond) elevate to values above their threshold levels and the photon density grows. But then, the stimulated emission rate also heightens that leads to reducing of the carrier density and gain until a new steady-state balance is created [10]. Differential gain, before the threshold gain, declines as the initial relaxation time increases and recombination times in QDs and WL decrease. In fact, enhancing the initial relaxation time and decreasing the recombination times result in increasing the threshold

current. A small decrease occurs at threshold gain for lower recombination time in WL. After threshold,differential gain is the same for different initial relaxation times and different recombination times in WL (Fig. 5(a) and Fig. 5(b)). Since relaxation oscillation frequency has square direct relation with differential gain [11], relaxation oscillation frequency and modulation bandwidth decrease as the initial relaxation time enhances and recombination times decrease. Fig. 5(c) shows that light amplification is linear beneath the lasing threshold.

CONCLUSION

Considering energy level and size distributions of self-assembled quantum-dots, we solved the rate equations numerically using fourth-order Runge-Kutta method andsimulated static-characteristics of InGaAs/GaAs SAQD-LD. Simulation results of the static-characteristics showed that slope efficiency elevates as the homogeneous broadening increases whereas it becomes equal to inhomogeneous broadening. Exceeding the homogeneous broadening from inhomogeneous broadening and elevating inhomogeneous broadening result in degradation of light-current characteristics. Threshold current increases as the homogeneous and inhomogeneous broadenings enhance. Nonlinearity appears in light-current characteristics whereas homogeneous broadening becomes equal to inhomogeneous broadening. This is the point that the SAQD laser has the best performance. In other words, the SAQD laser reveals its bestperformance when both homogeneous and inhomogeneous broadenings are the same. We also saw that increasing of homogeneous broadening from inhomogeneous broadening leads to declining of static-characteristics of InGaAs/GaAs SAQD-LD. We revealed that there is a threshold QD coverage and an optimum QD coverage in which the SAQD lasers operate with lowest possible threshold current and maximum output power. Optical gain increases to the threshold gain and then fixes as the injected current elevates. Differential gain also degrades as the initial relaxation time enhances and recombination times decrease, as a result, the relaxation oscillation frequency and modulation bandwidth degrade.

REFERENCES

1. Arakawa, Y. and H. Sakaki, 1982. Appl. Phys. Lett., 40: 939.
2. Bimberg, D., 1999. 'Quantum Dot Heterostructures', John Wiley & Sons Inc.,
3. Sugawara, M., 1998. 'Part of the SPIE Conference on Physics and Simulation of optoelectronic devises VI', 3283: 88.
4. Fiore, A. and A. Markus, 2007. IEEE J. Quantum Electron., 43: 3.
5. Sugawara, M., 2005. Appl. Phys., 97: 043523.
6. Sugawara, M., 2000. Phys. Rev. B., 61: 7595.
7. Sugawara, M., 1997. Applied. Phys. Lett., 71: 2791.
8. Tan, C.L., 2008. Comput. Mater. Sci., doi: 10.1016/j. commatsci. 01.049.
9. Tan, C.L. and Y. Wang, 2007. Applied Phys. Lett. 91: 061117.
10. Coldren, A., 1995. 'Diode Lasers and Photonic Integrated Circuits', John Wiley & Sons Inc.,
11. Sugawara, M., 1999. 'Self -Assembled InGaAs/GaAs Quantum Dots', Academic Press, pp: 60.